16th European Signal Processing Conference (EUSIPCO 2008), Lausanne, Switzerland, August 25-29, 2008, copyright by EURASIP

MULTILEAD ESTIMATION OF T-WAVE ALTERNANS IN THE ECG USING PRINCIPAL COMPONENT ANALYSIS

Violeta Monasterio, Pablo Laguna and Juan Pablo Martínez

CIBER-BBN, Communications Technologies Group, Aragon Institute of Engineering Research, University of Zaragoza
María de Luna,3. 50018, Zaragoza, Spain
email: violeta.monasterio@unizar.es

ABSTRACT

Several methods have been proposed to automatically detect and estimate T-wave alternans (TWA) in the electrocardiogram. All of them operate on a single-lead basis, and one major drawback is their low sensitivity to low-level alternans. Our group proposed a novel multilead TWA analysis scheme that combines Principal Component Analysis (PCA) with a technique based on the Generalized Likelihood Ratio Test (GLRT). In this work, we evaluate the estimation performance of the proposed scheme, and we compare it to a single-lead analysis scheme. Simulation results show that the proposed multilead scheme allows the estimation of TWA with a SNR 25 dB lower than a single-lead scheme for a given level of accuracy.

1. INTRODUCTION

The electrocardiogram (ECG) is extensively used as a clinical tool to study the heart function. ECG signals are measured placing electrodes on the body surface and recording the electrical activity of the heart. The simultaneous recording of the ECG on different chest locations (leads) allows a spatial perception of the cardiac events. The most widely used lead system in clinical practice is the standard 12-lead set. The ECG usually presents five characteristic waves on each beat, labeled from P to T (see Figure 1(a)). The time interval between the end of the S wave and the end of the T wave, known as ST-T segment, represents the repolarization activity of the heart ventricles.

T-wave alternans (TWA) is defined as a consistent fluctuation in the repolarization morphology on an every-other-beat basis (see Figure 1(b) and (c)). TWA is presently regarded as a promising index of susceptibility to sudden cardiac death [1, 2]. Several methods exist to automatically detect and estimate TWA [3]. All of them work on a single-lead basis. A major drawback of these methods is their low sensitivity to low-level alternans [2, 3].

In a previous work [4], we presented a multilead analysis scheme that combines Principal Component Analysis (PCA) and a technique based on the Generalized Likelihood Ratio Test (GLRT) [5, 6]. We evaluated the detection performance and compared it with a single-lead scheme. In this work we complete the characterization of the proposed multilead scheme by evaluating the estimation performance. To do so, we carry out a simulation study and compare the results with the single-lead scheme.

This paper is organized as follows. In Sections 2 and 3, we describe the TWA analysis schemes and the simulation study respectively. Section 4 shows the simulation results. In Section 5 we discuss the results, and in Section 6 we present the conclusions of this work.

2. TWA ANALYSIS

2.1 Multilead scheme

The block diagram of the proposed multilead scheme is shown in Figure 2. It consists of five stages: preprocessing, signal transformation with PCA, TWA detection, signal reconstruction and TWA estimation.

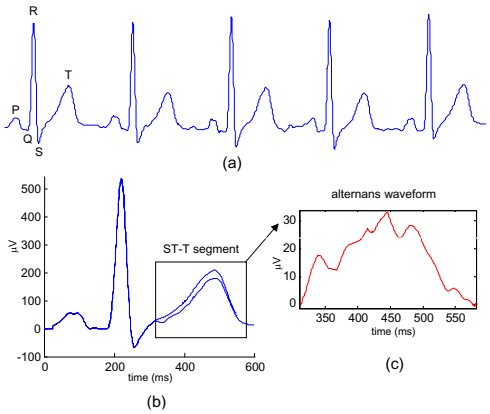

Figure 1: (a) ECG signal with visible TWA. (b) Superposition of two consecutive beats. (c) Alternans waveform.

2.1.1 *Preprocessing*

In the preprocessing stage, the multilead ECG signal is decimated to obtain a sampling frequency of 125 Hz, and low-pass filtered with a cut-off frequency of 20 Hz. Baseline wandering is removed using a cubic splines interpolation technique. Figure 3(a) shows an example. ST-T segments are then extracted.

Let K be the number of beats in the input signal, N the number of samples of each ST-T complex, L the number of leads, and $x_{k,l}(n)$ the ST-T complex of the k-th beat and the l-th lead. Each ST-T complex can be modeled as

$$x_{k,l}(n) = a_l(n)(-1)^k + s_l(n) + v_{k,l}(n) \quad n = 0 \ldots N-1$$

where $a_l(n)$ is the alternans waveform, $s_l(n)$ is the background ST-T complex, which is periodically repeated in each beat, and $v_{k,l}(n)$ is additive Laplacian noise. Complexes from the different leads are put together into a matrix $\mathbf{X}_k$

$$\mathbf{X}_k = \begin{bmatrix} \mathbf{x}_{k,1}^T \\ \ldots \\ \mathbf{x}_{k,L}^T \end{bmatrix} = \begin{bmatrix} x_{k,1}(0) & \ldots & x_{k,1}(N-1) \\ \ldots & \ldots & \ldots \\ x_{k,L}(0) & \ldots & x_{k,L}(N-1) \end{bmatrix} \quad (1)$$

The n-th column of $\mathbf{X}_k$ contains the amplitudes of the L leads at a given time. The $\mathbf{X}_k$ matrices are concatenated to form the data matrix $\mathbf{X}$

$$\mathbf{X} = [\mathbf{X}_0 \quad \mathbf{X}_1 \quad \ldots \quad \mathbf{X}_{K-1}] \quad (2)$$

The l-th row of $\mathbf{X}$ contains the concatenated ST-T complexes corresponding to the l-th lead.

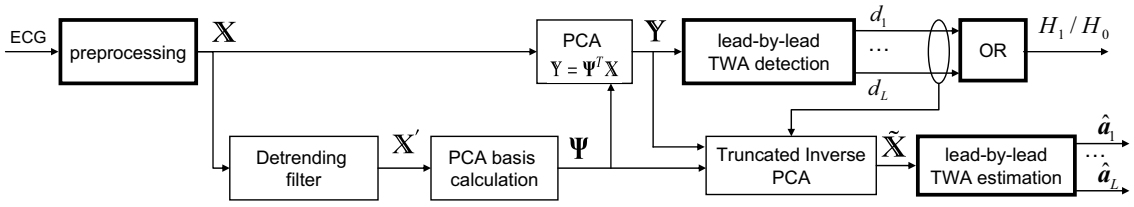

Figure 2: Block diagram of the multilead scheme. The blocks in bold line are the ones used in the single-lead scheme. Note that in the single-lead scheme $\mathbf{Y} = \mathbf{X} = \tilde{\mathbf{X}}$.

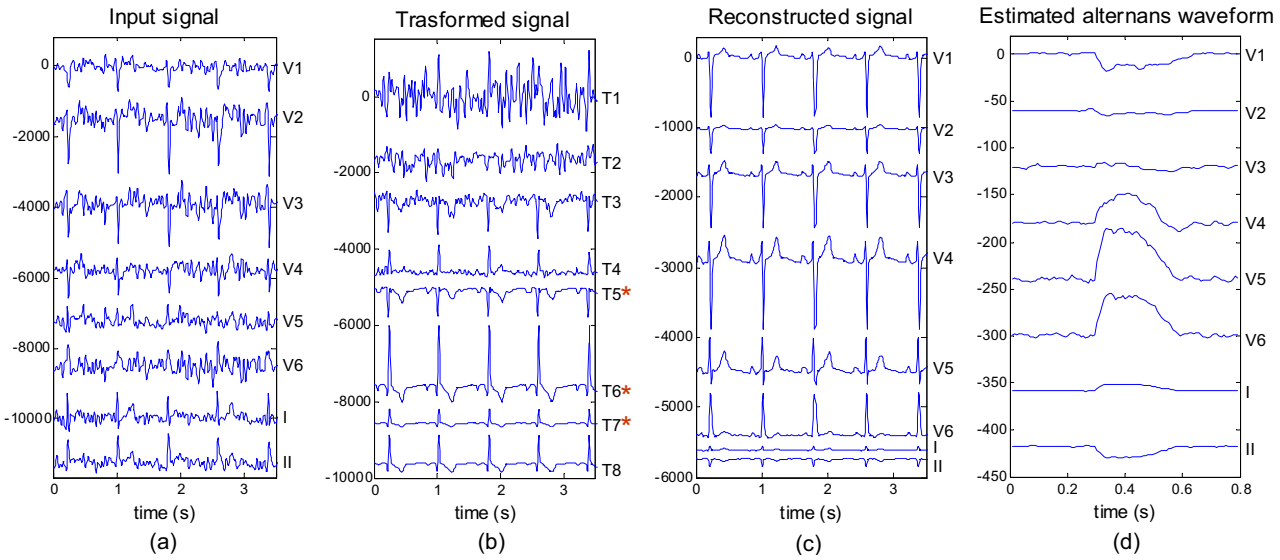

Figure 3: (a) Input signal with SNR $= -20$ dB. (b) Transformed signal after PCA. Asterisks indicate the leads where TWA is detected ($d_5 = d_6 = d_7 = 1$). (c) Reconstructed signal after truncated inverse PCA. (d) Estimated alternans waveform. Note that alternans is visible in T5, T6, and V4 to V6 in the reconstructed signal. Ordinate units in μV.

2.1.2 *Signal transformation with PCA*

After the preprocessing stage, a simple detrending filter cancels the background ST-T complex

$$\mathbf{x}'_{k,l} = 0.5\left(\mathbf{x}_{k,l} - \mathbf{x}_{k-1,l}\right),\ k = 1 \ldots K-1$$

The resulting detrended beats $\mathbf{x}'_{k,l}$ are piled and concatenated as in (1) and (2) to obtain a detrended data matrix $\mathbf{X}'$.

PCA is then applied. First, the interlead correlation matrix is estimated as

$$\hat{\mathbf{R}}_{\mathbf{X}'} = \frac{1}{LN}\mathbf{X}'\mathbf{X}'^T$$

Then, the eigenvector equation for $\hat{\mathbf{R}}_{\mathbf{X}'}$ is solved to obtain the whole set of L principal components of $\mathbf{X}'$

$$\hat{\mathbf{R}}_{\mathbf{X}'}\mathbf{\Psi} = \mathbf{\Psi}\mathbf{\Lambda}$$

thus obtaining the eigenvectors matrix $\mathbf{\Psi}$. Finally, an orthonormal linear transformation based on $\mathbf{\Psi}$ is applied

$$\mathbf{Y} = \mathbf{\Psi}^T\mathbf{X}$$

to obtain the transformed data matrix $\mathbf{Y}$. The l-th row of $\mathbf{Y}$ contains the transformed data corresponding to the l-th principal component, and from here on we will refer to it as the l-th transformed lead (Tl) for simplicity. Figure 3(b) shows the transformed signal.

2.1.3 *TWA detection*

To detect TWA in the transformed data, the GLRT is applied in each transformed lead as proposed in [5, 6]. The result of this lead-by-lead detection is denoted as d_l: if alternans is detected in the l-th transformed lead, $d_l = 1$, and $d_l = 0$ otherwise. The overall TWA detection is positive if alternans is detected at least in one transformed lead ('OR' block in Figure 2).

2.1.4 *Signal reconstruction with inverse PCA*

After TWA detection, and prior to the TWA estimation stage, a new signal in the original domain is reconstructed. Both principal components (columns in $\mathbf{\Psi}$) and transformed leads (rows in $\mathbf{Y}$) corresponding with l such that $d_l = 0$ are eliminated, thus obtaining the truncated basis matrix $\mathbf{\Psi}_{\text{TR}}$ and the truncated transformed data matrix $\mathbf{Y}_{\text{TR}}$ respectively. A reconstructed signal in the original domain is then obtained with the truncated matrices,

$$\tilde{\mathbf{X}} = \mathbf{\Psi}_{\text{TR}}\mathbf{Y}_{\text{TR}}$$

Figure 3(c) shows the reconstructed signal. Note that $\tilde{\mathbf{X}}$ is equivalent to a spatially filtered version of $\mathbf{X}$, where the aim of the equivalent filter is to preserve the alternans content, not to obtain a perfect reconstruction.

2.1.5 *TWA estimation*

The reconstructed data matrix $\tilde{\mathbf{X}}$ consists of the concatenation of the multilead single-beat matrices $\tilde{\mathbf{X}}_k$:

$$\tilde{\mathbf{X}} = \left[\tilde{\mathbf{X}}_0 \quad \tilde{\mathbf{X}}_1 \quad \ldots \quad \tilde{\mathbf{X}}_{K-1}\right]$$

where

$$\tilde{\mathbf{X}}_k = \begin{bmatrix} \tilde{\mathbf{x}}_{k,1}^T \\ \dots \\ \tilde{\mathbf{x}}_{k,L}^T \end{bmatrix}$$

with $\tilde{\mathbf{x}}_{k,l}$ corresponding to the reconstructed ST-T complex of the k-th beat in the l-th lead. To estimate the alternans waveform and amplitude, the Maximum Likelihood Estimation for Laplacian noise (Laplacian MLE) is applied to the reconstructed data as proposed in [5, 6]. Note that TWA estimation is only possible when a reconstructed signal is available, that is, when the overall detection is positive. Figure 3(d) shows an example of estimated alternans.

2.2 Single-lead scheme

The single-lead scheme handles each lead independently throughout the process. It consists of the same preprocessing, TWA estimation and TWA detection stages as the multilead scheme, but without the intermediate PCA processing. That is, with the single-lead scheme $\mathbf{Y} = \mathbf{X} = \tilde{\mathbf{X}}$. The stages of the single-lead scheme are shown in bold in Figure 2. Note that this scheme always produces a TWA estimation, regardless of the detection result.

3. SIMULATION STUDY

We carried out a simulation study to evaluate the multilead scheme and to compare it with the single-lead scheme. Figure 4 shows the simulation setup. We simulated multilead ECG signals by adding noise and TWA to a clean background ECG.

For the background ECG we selected a standard beat from a 12-lead record and repeated it $K = 32$ times. We estimated and extracted an alternans waveform from another 12-lead record, using the GLRT method as described in [6]. Both records belonged to the STAFF-III database [6]. From the 12-lead set, we only selected the eight leads that are linearly independent, that is, leads V1 to V6, I and II ($L = 8$). We added Gaussian noise to the sum of the background ECG and alternans. For each realization, we simulated L segments of noise of $K \times N$ samples. We normalized each segment so that its root mean square (RMS) value was 1 μV.

Let $\mathbf{W}$ be the multilead noise matrix formed by the noise segments $\mathbf{w}_l$,

$$\mathbf{W} = \begin{bmatrix} \mathbf{w}_1^T \\ \dots \\ \mathbf{w}_L^T \end{bmatrix} \tag{3}$$

Noise segments $\mathbf{w}_l$ are spatially uncorrelated, i.e.

$$\hat{\mathbf{R}}_W = \frac{1}{NL}\mathbf{W}\mathbf{W}^T = \mathbb{I} \tag{4}$$

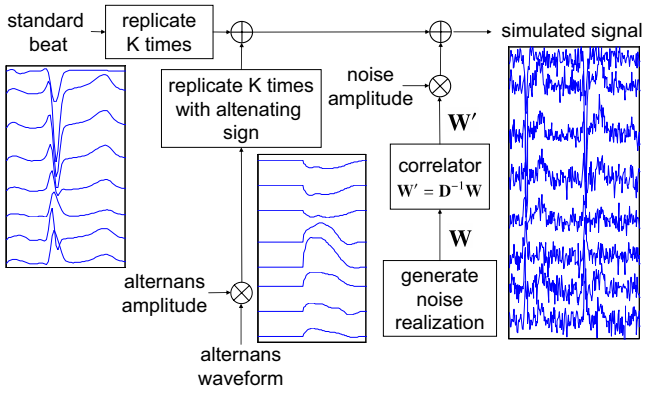

Figure 4: Simulation of ECG signals with TWA and noise. Signals scale not preserved for better visualization.

However, in real ECG records the noise in the different leads is not uncorrelated. To simulate a physiological-like correlation, we selected 2000 segments of noise for each lead from 10 records of the PTB Diagnostic ECG database [7]. For each segment, the 50 ms interval prior to a P wave onset was selected, and DC level was removed. Segments corresponding to each lead were concatenated, and the resulting noise leads were piled similarly to (3) to form a noise matrix $\mathbf{N}$. The interlead correlation matrix of $\mathbf{N}$ was estimated similarly to (4). Applying the Cholesky decomposition to its inverse we obtained

$$\hat{\mathbf{R}}_N^{-1} = \mathbf{D}\mathbf{D}^T$$

where $\mathbf{D}$ is an upper triangular matrix with strictly positive diagonal entries. The inverse of $\mathbf{D}$ was used to correlate spatially the generated noise

$$\mathbf{W}' = \mathbf{D}^{-1}\mathbf{W}$$

thus obtaining a noise matrix $\mathbf{W}'$ whose interlead correlation equals $\hat{\mathbf{R}}_N$. Finally, the noise was scaled so that the RMS value of the least noisy lead was 200 μV. Alternans was then scaled to obtain a desired value of SNR, defined as the ratio between alternans power and noise power.

We simulated multilead ECG signals with SNR values ranging from -60 to 10 dB, and also without TWA. For each parameter combination, we generated 10^4 noise realizations. We processed the signals with both the single-lead and the multilead schemes and compared the results.

4. RESULTS

After processing the simulated signals with both schemes, we studied the detection performance and the accuracy of the estimation. Detection results were reported in a previous work [4]. Therefore, in this section we will only present those that are relevant to the study of the estimation performance. To evaluate the detection performance, we selected a fixed value for the threshold to obtain a probability of false alarm $P_{FA} = 0.01$, and compared the resulting detection probability P_D. Figure 5 shows the detection behavior of the schemes for different values of SNR.

In this study, our aim was to evaluate the accuracy of the estimation as independently from the detection as possible. Comparing both schemes was not straightforward: the single-lead scheme always produces an estimation of the alternans, regardless of the detection result; however, the multilead scheme only produces an estimation when the detection is positive. Therefore, we considered the results of the 10^4 realizations for both schemes as follows: if detection was positive, the output of the estimation stage was taken directly; if detection was negative, a zero signal was taken for the eight leads.

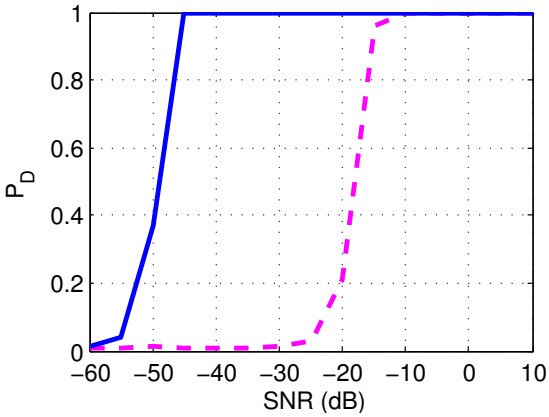

Figure 5: P_D for $P_{FA} = 0.01$ of the multilead (solid line) and the single-lead scheme (dashed line) vs. SNR.

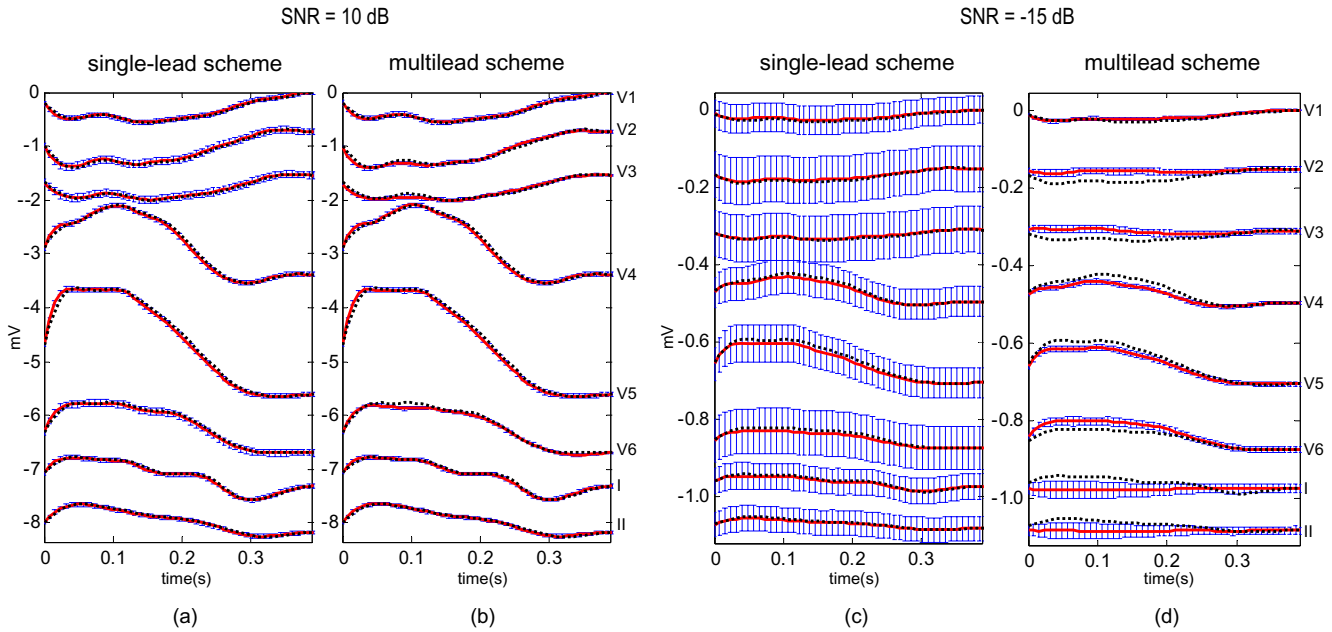

Figure 6: Expected value (red line) and standard deviation (blue bars) of the estimated alternans waveforms, obtained with (a) the single-lead and (b) the multilead scheme for SNR = 10 dB, and with (c) the single-lead and (d) the multilead scheme for SNR = -15 dB. True alternans shown in black dashed line. Leads offset included for better visualization.

We evaluated the estimation performance of the two schemes in terms of bias, variance and mean square error. Let us denote by $\hat{a}_l(n)$ the n-th sample of the estimated alternans waveform in the l-th lead, and by $a_l(n)$ the same sample of the true alternans waveform. For each value of SNR, we estimated $E\{\hat{a}_l(n)\}$ as the average of $\hat{a}_l(n)$ in the 10^4 realizations. Figure 6 shows the expected value and the standard deviation of the estimation for both schemes and for different values of SNR.

For each SNR value and each lead l, we computed the bias and the error of the estimation as

$$b_l(n) = E\{\hat{a}_l(n)\} - a_l(n),\ n = 0 \ldots N-1$$

$$e_l^2(n) = E\left\{(\hat{a}_l(n) - a_l(n))^2\right\},\ n = 0 \ldots N-1$$

As before, the expected values were estimated as the average of the 10^4 realizations . Then, we defined two performance parameters:

$$\mathscr{R}_{b_l}(\%) = \frac{\sqrt{\frac{1}{N}\sum_{n=0}^{N-1} b_l^2(n)}}{\sqrt{\frac{1}{N}\sum_{n=0}^{N-1} a_l^2(n)}} \times 100$$

$$\mathscr{R}_{e_l}(\%) = \frac{\sqrt{\frac{1}{N}\sum_{n=0}^{N-1} e_l^2(n)}}{\sqrt{\frac{1}{N}\sum_{n=0}^{N-1} a_l^2(n)}} \times 100$$

The parameter $\mathscr{R}_{b_l}$ measures the relative bias of the estimation in the l-th lead. Figure 7 shows the evolution of $\mathscr{R}_{b_l}$ vs. SNR for the two schemes. The parameter $\mathscr{R}_{e_l}$ measures the relative error caused by both the bias and the variance of the estimation. It is plotted vs. SNR in Figure 8.

5. DISCUSSION

In Figure 6, we can observe that the bias of the multilead estimation is higher than the bias of single-lead estimation in both cases. Indeed, Figure 7 shows that the bias of the multilead estimation is higher for SNR $\geq$ -15 dB. This is due to the truncation carried out in the reconstruction stage. As only a subset of transformed leads is used to reconstruct the signal, the reconstructed alternans lacks the content of the truncated leads. On the other hand, when SNR $<$ -15 dB the relative bias of the single-lead estimation tends to 100% for all the leads, that is, the estimation tends to zero. This is so because, at SNR = -15dB, the P_D of the single-lead scheme starts decreasing (see Figure 5), so we are considering more and more realizations to be zero. In this case the behavior of the multilead scheme is better. For low SNR levels, the relative bias of the multilead estimation varies differently for each lead, and for some of them it is $< 50\%$ until SNR = -45dB.

In Figure 6 we can also see that the variance of the multilead estimation is lower than the variance of the single-lead estimation in all the leads. This lower variance compensates the bias of the multilead estimation, so the final relative error $\mathscr{R}_{e_l}$ is equal or lower than the error of the single-lead estimation for all SNR values. This is shown in Figure 8. For high levels of SNR, $\mathscr{R}_{e_l}$ is similar for both schemes, and for low SNR levels the $\mathscr{R}_{e_l}$ of the multilead estimation is lower. In particular, when SNR $<$ -15 dB, $\mathscr{R}_{e_l} > 100\%$ in the eight leads for the single-lead estimation, whereas with the multilead estimation such degradation does not appear until SNR $<$ -40 dB.

6. CONCLUSIONS

According to simulation results, the proposed multilead scheme improves significantly the estimation of TWA, specially at low SNR levels. With the multilead scheme we can estimate TWA with a SNR 25 dB lower than with a single-lead scheme for a given level of accuracy. Although further validation with real signals is needed, the proposed scheme may find application in noisy signals such as stress test ECG, wich is one of the main clinical scenarios where TWA analysis is performed.

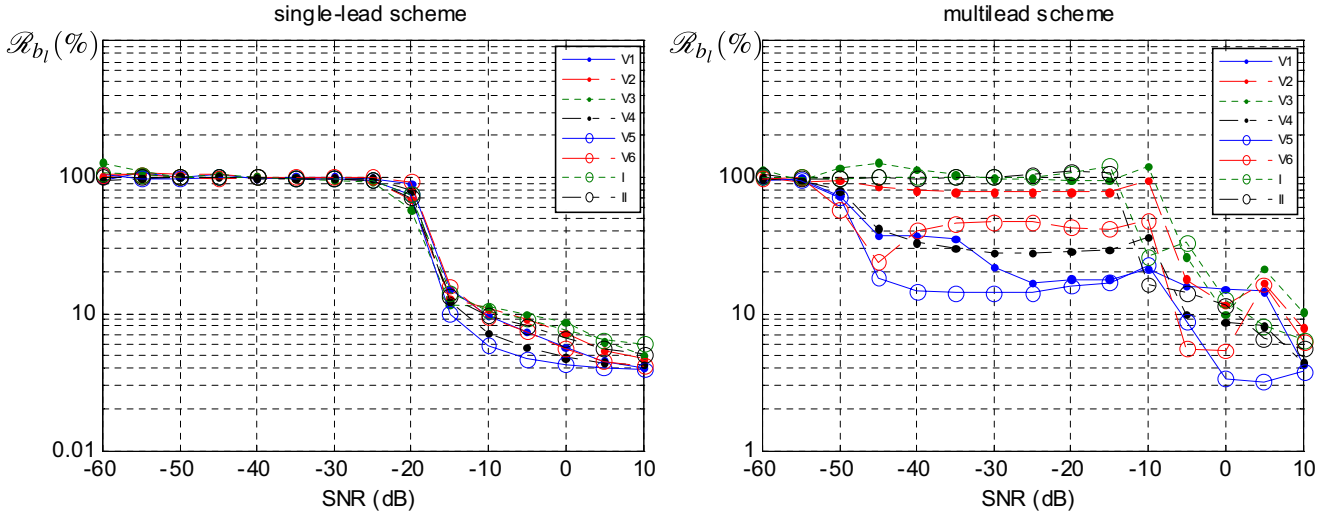

Figure 7: Relative bias of the alternans estimation for the single-lead (left) and the multilead scheme (right) vs. SNR

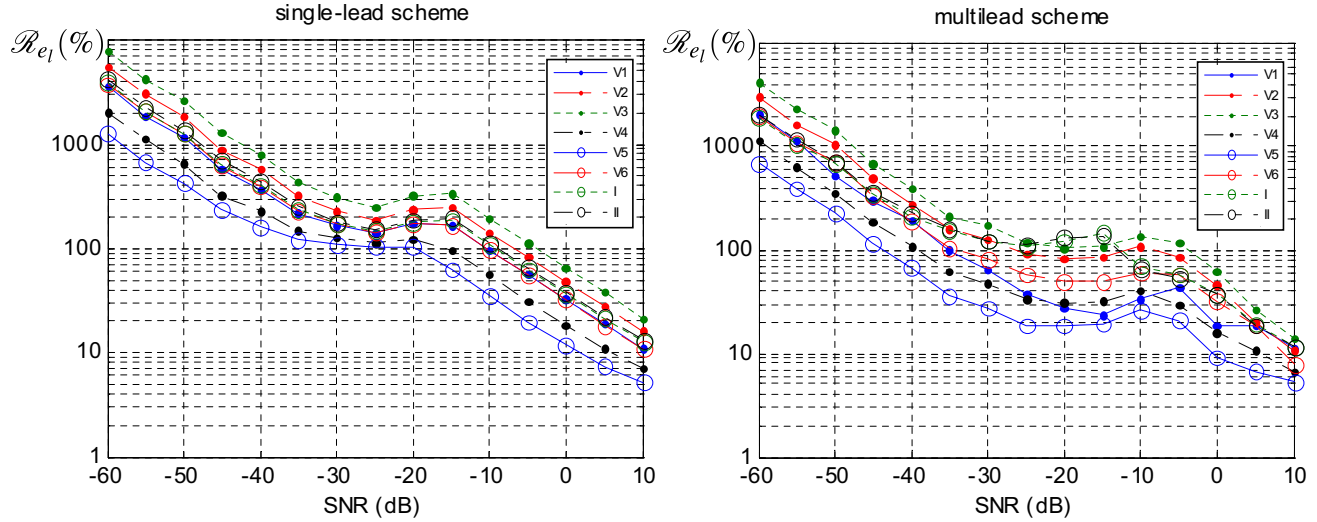

Figure 8: Relative error of the alternans estimation for the single-lead (left) and the multilead scheme (right) vs. SNR

Acknowledgments

This work was supported by CIBER-BBN through ISCIII, TEC-2007-68076-C02-02 from CICYT, and GTC T-30 from DGA (Spain).

REFERENCES

[1] Rosenbaum DS, Jackson LE, Smith JM, Garan H, Ruskin JN, Cohen RJ. Electrical Alternans and Vulnerability to Ventricular Arrhythmias. N Engl J Med 1994;330(4):235–241.

[2] Narayan SM. "T-Wave Alternans and the Susceptibility to Ventricular Arrhythmias". J Am Coll Cardiol 2006;47(2):269–281.

[3] Martínez JP, Olmos S. "Methodological principles of T wave alternans analysis: a unified framework". IEEE Trans Biomed Eng 2005;52:599–613.

[4] Monasterio V, Martínez JP. "A multilead approach to T-wave alternans detection combining Principal Component Analysis and the Laplacian Likelihood Ratio method". In Computers in Cardiology 2007; 34:5–8.

[5] Martínez JP, Olmos S. "A Robust T-Wave Alternans Detector Based On The GLRT For Laplacian Noise Distribution". In Computers in Cardiology 2002, volume 29. IEEE Comp. Soc. Press, 2002; 677–680.

[6] Martínez JP, Olmos S, Wagner G, Laguna P. "Characterization of repolarization alternans during ischemia: time-course and spatial analysis". IEEE Trans Biomed Eng 2006;53:701–711.

[7] Bousseljot R, Kreiseler D, Schnabel A. "Nutzung der EKG-Signaldatenbank CARDIODAT der PTB über das Internet". Biomedizinische Technik 1995;40:317–318.